the plant journal

SEB Society for Experimental Biology

The Plant Journal (2016) **85,** 219–228 doi: 10.1111/tpj.13101

Effect of *Chlamydomonas* plastid terminal oxidase 1 expressed in tobacco on photosynthetic electron transfer

Kathleen Feilke[1], Peter Streb[2], Gabriel Cornic[2], François Perreau[3,4], Jerzy Kruk[5] and Anja Krieger-Liszkay[1,*]

[1]*Institute for Integrative Biology of the Cell (I2BC), Commissariat à l'Energie Atomique et aux Energies Alternatives (CEA) Saclay, Institut de Biologie et de Technologie de Saclay, Centre National de la Recherche Scientifique (CNRS), Université Paris-Sud, Université Paris-Saclay, 91191 Gif-sur-Yvette Cedex, France,*

[2]*Ecologie, Systématique et Evolution, Université Paris-Sud, Université Paris-Saclay, UMR-CNRS 8079, Bâtiment 362, 91405 Orsay Cedex, France,*

[3]*Institut Jean-Pierre Bourgin, INRA, UMR 1318, ERL CNRS 3559, Saclay Plant Sciences, RD10, F-78026 Versailles, France,*

[4]*Institut Jean-Pierre Bourgin, AgroParisTech, UMR 1318, ERL CNRS 3559, Saclay Plant Sciences, RD10, F-78026 Versailles, France, and*

[5]*Department of Plant Physiology and Biochemistry, Faculty of Biochemistry, Biophysics and Biotechnology, Jagiellonian University, Gronostajowa 7, 30-387 Kraków, Poland*

Received 3 August 2015; revised 23 November 2015; accepted 25 November 2015; published online 14 December 2015.
*For correspondence (e-mail anja.krieger-liszkay@cea.fr).

SUMMARY

The plastid terminal oxidase PTOX is a plastohydroquinone:oxygen oxidoreductase that is important for carotenoid biosynthesis and plastid development. Its role in photosynthesis is controversially discussed. Under a number of abiotic stress conditions, the protein level of PTOX increases. PTOX is thought to act as a safety valve under high light protecting the photosynthetic apparatus against photodamage. However, transformants with high PTOX level were reported to suffer from photoinhibition. To analyze the effect of PTOX on the photosynthetic electron transport, tobacco expressing PTOX-1 from *Chlamydomonas reinhardtii* (Cr-PTOX1) was studied by chlorophyll fluorescence, thermoluminescence, P700 absorption kinetics and CO_2 assimilation. Cr-PTOX1 was shown to compete very efficiently with the photosynthetic electron transport for PQH_2. High pressure liquid chromatography (HPLC) analysis confirmed that the PQ pool was highly oxidized in the transformant. Immunoblots showed that, in the wild-type, PTOX was associated with the thylakoid membrane only at a relatively alkaline pH value while it was detached from the membrane at neutral pH. We present a model proposing that PTOX associates with the membrane and oxidizes PQH_2 only when the oxidation of PQH_2 by the cytochrome b_6f complex is limiting forward electron transport due to a high proton gradient across the thylakoid membrane.

Keywords: plastid terminal oxidase, photosynthetic electron transport, photooxidative stress, regulation, *Nicotiana tabacum*, *Chlamydomonas reinhardtii* PTOX1.

INTRODUCTION

The plastid terminal oxidase PTOX is found in plants, green algae and cyanobacteria. It is a plastohydroquinone: oxygen oxidoreductase (Kuntz, 2004; Rumeau *et al.*, 2007) that shares structural similarities with alternative oxidase AOX found in plant mitochondria. Both belong to the non-heme diiron carboxylate family (Berthold *et al.*, 2000; Fu *et al.*, 2005).

Plastid terminal oxidase (PTOX) was discovered in the so-called *immutans* of *A. thaliana* showing a variegated phenotype (Wetzel *et al.*, 1994; Carol *et al.*, 1999; Wu *et al.*, 1999). In chloroplasts, PTOX is located at the stroma lamellae facing the stroma (Lennon *et al.*, 2003). PTOX is involved in carotenoid synthesis during plastid development (Carol *et al.*, 1999; Wu *et al.*, 1999), in which it reoxidizes plastoquinol (PQH_2) and provides plastoquinone (PQ) as electron acceptor for phytoene desaturation reactions. Moreover, PTOX has been shown to be involved in chlororespiration (Aluru and Rodermel, 2004; Shahbazi *et al.*, 2007) together with the NADPH dehydrogenase (ndh) complex. Despite recent increase of knowledge on a biochemical level (Josse *et al.*, 2003; Yu *et al.*, 2014), the physiological role of PTOX during photosynthesis remains

less clear. Increased level of PTOX are found in plants exposed to abiotic stress as high temperatures, high light and drought (Quiles, 2006; Díaz *et al.*, 2007; Ibáñez *et al.*, 2010), low temperatures and high light (Ivanov *et al.*, 2012), salinity (Stepien and Johnson, 2009) and in alpine plants at low temperature and high UV exposure (Streb *et al.*, 2005; Laureau *et al.*, 2013), and it has been proposed that PTOX acts as a safety valve in the light under abiotic stress conditions by protecting the plastoquinol pool from over-reduction. A highly reduced PQ pool hinders forward electron flow and triggers charge recombination reaction in photosystem (PS) II leading to the generation of triplet chlorophyll and the highly toxic singlet oxygen (Krieger-Liszkay, 2005). However, overexpression of PTOX in *A. thaliana* did not protect against light-induced photodamage (Rosso *et al.*, 2006). Tobacco expressing, in addition to its endogenous PTOX, PTOX from *A. thaliana* (Joët *et al.*, 2002; Heyno *et al.*, 2009) or from *C. reinhardtii* (Ahmad *et al.*, 2012) showed even stronger photoinhibition and elevated reactive oxygen species (ROS) production (Heyno *et al.*, 2009).

The aim of the present work was to study the efficiency of PQH_2 oxidation by PTOX in comparison to forward electron flow and the regulation of PTOX activity. The endogenous PTOX level in non-stressed plants is very low (1% of PSII levels in *Arabidopsis thaliana;* Lennon *et al.*, 2003), which makes it difficult to study the activity of this enzyme *in vivo* under steady-state conditions. Therefore, we chose tobacco expressing PTOX1 from *Chlamydomonas reinhardtii* (Ahmad *et al.*, 2012), which shows among the available transformants the highest PTOX activity and the strongest phenotype. PTOX activity and its effect on photosynthetic electron transport were followed by chlorophyll fluorescence, thermoluminescence, P700 absorption changes and CO_2 assimilation. Based on immunoblotting results we propose a model suggesting that in wild-type plants PTOX is only operational when the photosynthetic electron transport is limited by a high pH gradient across the thylakoid membrane.

RESULTS

Cr-PTOX1 phenotype under different light conditions

Tobacco expressing *C. reinhardtii* PTOX1 (Cr-PTOX1) was grown under continuous white light at an intensity of 80 μmol photons m^{-2} sec^{-1} or under a photoperiod of 12 h light/12 h dark at 80 μmol photons m^{-2} sec^{-1} (Figure S1a). At 80 μmol photons m^{-2} sec^{-1} growth was highly affected in Cr-PTOX1 plants (leaf size from equivalent developmental stage about 30% of wild-type) when grown under a light/dark photoperiod. Under continuous light (80 μmol photons m^{-2} sec^{-1}) growth was less, but still strongly retarded (leaf size about 50% of wild-type). Since Cr-PTOX1 plants grew best under this condition, the following experiments were performed on plants grown under continuous light. Higher light intensities of 125 μmol photons m^{-2} sec^{-1} cause severe light stress in Cr-PTOX1 plants (Ahmad *et al.*, 2012). In accordance with Ahmad *et al.* (2012), the maximum quantum efficiency of PSII (F_v/F_m) was significantly lower in Cr-PTOX1 plants even when grown under continuous light (Table 1 and Figure S2). Images of chlorophyll fluorescence on whole plants show that the maximum quantum efficiency of PSII was the same in all leaves of wild-type, while it was very heterogeneous in Cr-PTOX1 plants depending strongly on leaf age and area (Figure S1b) with the youngest leaves showing the lowest F_v/F_m ratio. Accordingly, the effective quantum yield of PSII [Φ(II)] was lower. Photochemical quenching, qP, was about half in Cr-PTOX1 plants compared with wild-type when leaves were illuminated with

Table 1 Comparison of pigment content, photosynthetic activity and fluorescence parameters between wild-type and Cr-PTOX1 plants

	Wild-type	Cr-PTOX1 plants
Chl *a* content (nmol g^{-1} dry weight)		
Chl *a* absolute	6097.7 ± 100.4	4117.1 ± 94.9
Pigment content (mmol mol^{-1} Chl *a*)		
Chl *a*	1000	1000
Chl *b*	353.0 ± 18.6	358.6 ± 3.7
β-Carotene	108.1 ± 9.6	86.9 ± 2.2
Zeaxanthin	11.4 ± 2.4	10.3 ± 1.5
cis-Violaxanthin	7.2 ± 2.4	24.7 ± 4.8
trans-Violaxanthin	42.2 ± 7.8	108.6 ± 5.5
cis -Neoxanthin	43.6 ± 1.8	45.5 ± 0.9
Lutein	182.5 ± 11.2	177.9 ± 1.2
PSI and PSII activity (μmol O_2 mg Chl^{-1} h^{-1})		
PSI	111.0 ± 15.0	100.0 ± 10.0
PSII	280.0 ± 50.0	240.0 ± 60.0
Chlorophyll fluorescence, *I* = 95 μmol photons m^{-2} sec^{-1}		
F_v/F_m	0.82 ± 0.011	0.67 ± 0.063
Φ_{PSII}	0.296 ± 0.014	0.133 ± 0.022
qP	0.455 ± 0.055	0.244 ± 0.046
NPQ	0.222 ± 0.029	0.305 ± 0.091
Chlorophyll fluorescence, *I* = 340 μmol photons m^{-2} sec^{-1}		
Φ_{PSII}	0.113 ± 0.008	0.016 ± 0.007
qP	0.236 ± 0.049	0.026 ± 0.018
NPQ	0.311 ± 0.022	0.519 ± 0.132
77 K fluorescence emission		
PSI/PSII	2.31 ± 0.41	2.25 ± 0.58

Chlorophyll and carotenoid content of mature leaves from wild-type and Cr-PTOX1 plants grown under continuous light at 80 μmol photons m^{-2} sec^{-1} were obtained by pigment extraction with HPLC. For better comparison values were normalized to Chl *a*. Individual plants were measured [*n* = 4 ± standard error (SE)]. PSII and PSI activities of thylakoid membranes were determined with the oxygen electrode (*n* = 3 ± SE). Chlorophyll fluorescence quenching analysis was performed *in vivo* with the DUAL-PAM at 95 and 340 μmol photons m^{-2} sec^{-1} on dark-adapted plants (*n* = 5 ± SE). 77K fluorescence emission spectra were measured after far-red illumination of the leaves (*n* = 5 ± SE).

95 μmol photons m^{-2} sec^{-1} and almost zero when higher light (340 μmol photons m^{-2} sec^{-1}) was applied. To investigate whether expression of Cr-PTOX1 led to more ROS, $O_2^{\bullet-}$/H_2O_2-derived hydroxyl radicals were measured using 4-POBN/EtOH/Fe-EDTA as spin-trapping assay (Heyno *et al.*, 2009). Leaf disks of Cr-PTOX1 plants incubated at growth or high light (500 μmol photons m^{-2} sec^{-1}) showed a higher ROS production than those of wild-type (Figure S3), indicating that expression of Cr-PTOX1 led to higher oxidative stress that is probably responsible for the photoinhibition observed in these plants (Ahmad *et al.*, 2012). To show that the photosystems were unaltered, the activity of PSI and PSII was determined using isolated thylakoid membranes and artificial electron acceptors to exclude that the expression of Cr-PTOX1 perturbed the photosynthetic machinery per se. As shown in Table 1, no significant difference was observed neither for the activity of PSI nor of PSII. Moreover, the PSI/PSII emission ratios determined by 77 K Fluorescence of Cr-PTOX1 plants are similar to those of the wild-type (Table 1 and Figure S4). Additionally, immunoblots showed no significant changes in the protein levels of the subunits PsbA and PsbS of PSII and of the large subunit of RubisCO (RbcL) in Cr-PTOX1 plants (Figure S5).

Cr-PTOX1 chlorophyll and carotenoid content

As Cr-PTOX1 is supposed to be involved in carotenoid synthesis of *C. reinhardtii* (Houille-Vernes *et al.*, 2011) providing oxidized plastoquinone as electron acceptor for the desaturation reactions of phytoene and as the leaves from Cr-PTOX1 plants were rather pale, the pigment content was determined. Pigment analysis showed that the chlorophyll (Chl) content decreased significantly in Cr-PTOX1 plants, with Chl *b* showing a decrease of 30% and Chl *a* of 35%. The total carotenoid content did not differ significantly between wild-type and Cr-PTOX1 plants (2.6 ± 0.5 μg mg^{-1} dry weight in wild-type as compared with 2.4 ± 0.1 μg mg^{-1} dry weight in Cr-PTOX1 plants), however, the β-carotene level decreased by about 19% when normalized to Chl *a* (Table 1) while the total level of violaxanthin increased in Cr-PTOX1 plants. The amount of *trans*-violaxanthin, the isomer involved in the xanthophyll cycle and non-photochemical quenching (NPQ), was about two times higher in Cr-PTOX1 plants (Table 1) in accordance with the high value for NPQ. The amount of *cis*-violaxanthin that serves as a precursor for abscisic acid (ABA) synthesis (Nambara and Marion-Poll, 2005) was increased by about three times.

Cr-PTOX1 and the redox state of the PQ pool

The question arises whether the additional PTOX activity in Cr-PTOX1 plants alters the redox state of the PQ pool. To investigate PTOX activity in Cr-PTOX1 plants, chlorophyll fluorescence induction curves were measured in thylakoids from wild-type and Cr-PTOX1 plants. The maximum level of fluorescence is reached when Q_A is in its reduced state. The induction of the fluorescence rise was slowed down in thylakoids from Cr-PTOX1 plants (Figure 1b), showing that the quinone reduction is slower due to higher PTOX activity. This was only seen at low light intensities (less than 60 μmol photons m^{-2} sec^{-1}). In the presence of DCMU, an inhibitor that binds to the Q_B binding pocket, no difference between Cr-PTOX1 and wild-type was any longer observed (Figure 1a,b). Addition of the inhibitor octylgallate also abolished the difference between thylakoids from Cr-PTOX1 plants and wild-type (not shown, but see Feilke *et al.*, 2014).

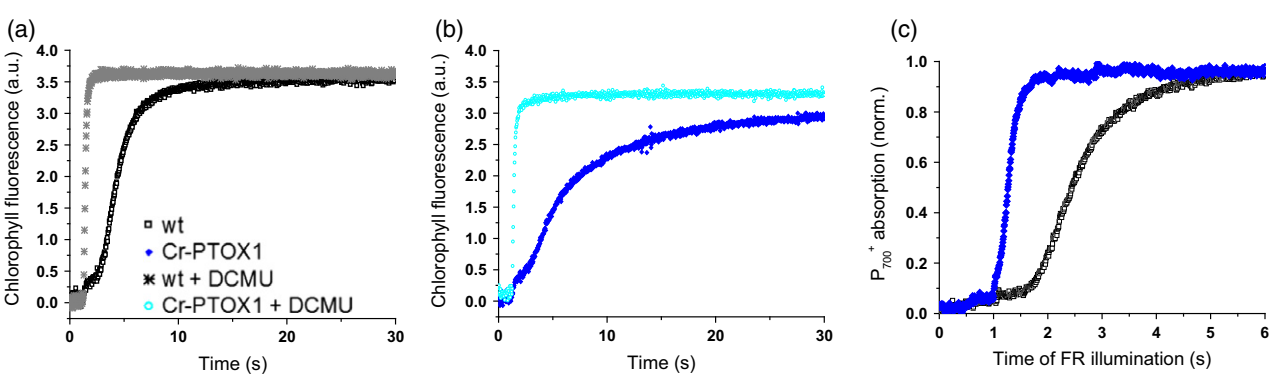

Figure 1. PTOX activity is increased in Cr-PTOX1 plants.
(a, b) Chlorophyll fluorescence induction curves of thylakoid membranes from (a) wild-type (open squares) and (b) Cr-PTOX1 (diamonds) plants. First, samples were measured in the absence of DCMU. Then DCMU was added to both samples after 5 min dark adaptation and the measurement was repeated (a, grey crosses: wild-type; b, circles: Cr-PTOX1). The light intensity was 22 μmol photons m^{-2} sec^{-1}. The variable part of the fluorescence of representative curves is shown. Measurements were performed with 20 μg Chl mL^{-1}.
(c) P_{700} oxidation in leaves of wild-type and Cr-PTOX1 plants. PSI oxidation was probed by far-red illumination of wild-type (black squares) and Cr-PTOX1 (diamonds) plants according to Joliot and Johnson (2011). Plants were dark adapted for 10 min. Then leaves were illuminated 5 min with far-red light, followed by 5 sec actinic red light (600 μmol photons m^{-2} sec^{-1}), 2 sec dark, 17 sec far-red light (I = 480 μmol photons m^{-2} sec^{-1}). Only the first seconds after onset of far-red light of representative curves are shown. The amplitudes of the signal were normalized to 1.

When PTOX activity is high, the reduction state of the PQ pool is expected to be low and the electron donation to PSI may become limiting. Absorption measurements at 830 nm were performed to follow P_{700} oxidation by FR illumination (Figure 1c). P_{700} was much faster oxidized in Cr-PTOX1 plants than in wild-type demonstrating that fewer electrons were available for reducing P_{700}^{+}, thereby indicating that the PQ pool was more oxidized in Cr-PTOX1 plants. Alternatively, the oxidation state of the PQ pool can be monitored by thermoluminescence. The intensity of the afterglow band (AG-band) band depends on the redox state of the PQ pool and of Q_B (Roncel and Ortega, 2005). As shown in Figure 2(a), the maximum temperature of the AG-band in Cr-PTOX1 leaves was almost the same as in wild-type while the intensity was drastically reduced indicating a high oxidation level of the PQ pool in Cr-PTOX1 plants. After excitation with a single-turnover flash, the B-band (reflecting $S_{2,3}Q_B^-$ charge recombination reactions) was obtained in both samples, showing that PSII functioned normally in Cr-PTOX1 plants (Figure 2b). Illumination with three single-turnover flashes leads to the induction of both, the B- and the AG-band (Krieger *et al.*, 1998) as seen for the wild-type in Figure 2(c). The glow curve of Cr-PTOX leaves from plants that had been dark-adapted for 2 min was dominated by the B-band. However, when Cr-PTOX1 plants were dark-adapted for at least 30 min the AG-band reappeared and the difference to the wild-type was no longer observed (Figure 2c). This indicates that PTOX activity is lost in Cr-PTOX1 expressing plants after prolonged dark adaptation.

To show in an independent way that the PQ pool was indeed more oxidized in Cr-PTOX1 plants, the redox state of the PQ pool was analyzed by high pressure liquid chromatography (HPLC) (Kruk and Karpinski, 2006). The PQ pool in leaves taken from growth light was significantly more oxidized in Cr-PTOX1 plants than in wild-type, and the size of the photochemically active PQ pool was reduced (Table 2). A smaller size of the PQ pool may limit photosynthetic electron flow as reflected by the low qP value in the Cr-PTOX1 plants. In contrast, the total PQ content was increased in Cr-PTOX1 plants, and most PQ was found in the photochemically non-active plastoquinone fraction localized in plastoglobuli, which was also more oxidized than in the wild-type. A decrease in the size of the active PQ pool and an increase in the PQ content in plastoglobuli was already shown previously for plants under different stress conditions (Nordby and Yelenosky, 1985; Hernández *et al.*, 1993; Munné-Bosch and Alegre, 2002). Besides the function in electron transfer in thylakoids, PQH_2 serves as the main lipophilic ROS scavenger in chloroplasts (Szymańska and Kruk, 2010).

Cr-PTOX1 plants show a more oxidized PQ pool, and higher PTOX activity might compete with cytochrome b_6f for the substrate PQH_2 under steady-state conditions. To obtain information of Cr-PTOX1 activity during steady-state photosynthesis saturation pulse analysis was used to determine PSI quantum yields at different light intensities. PSI quantum yield is dependent on both, donor-side and acceptor-side limitation. P_{700} of Cr-PTOX1 plants show at light intensities higher than 75 μmol photons m^{-2} sec^{-1} a significantly higher donor-side limitation Y(ND) than wild-type (Figure 3), indicating PTOX activity under steady-state conditions.

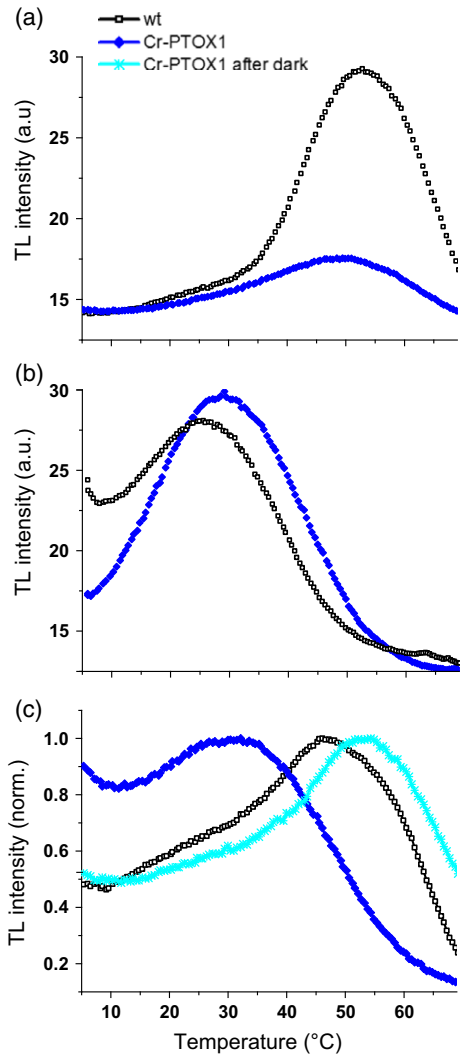

Figure 2. Thermoluminescence curves show a lower re-reduction of the PQ pool in the dark in Cr-PTOX1 plants.
(a) Two minutes dark-adapted leaves were illuminated 30 sec with far-red light (I = 480 μmol quanta m^{-2} sec^{-1}).
(b) Dark-adapted leaves were excited by one saturating single-turnover flash.
(c) Dark-adapted leaves were excited by three saturating single-turnover flashes. Open squares: wild-type leaf; diamonds: Cr-PTOX1 leaf; stars: Cr-PTOX1 leaf after 30 min dark incubation. Leaves from the light (80 μmol photons m^{-2} sec^{-1}) were 2 min dark-adapted prior to the excitation.

Table 2 Determination of the oxidation state of the PQ pool in wild-type and Cr-PTOX1 plants

	Wild-type	Cr-PTOX1
% reduction of PQ pool at growth light	99.1 ± 1.9	54.0 ± 3.1
% reduction of PQ photochemically non-active	90.8 ± 3.8	71.4 ± 5.2
Size of PQ pool (% of total PQ)	24.0 ± 2.4	8.7 ± 4.0
PQ_{total} (oxidized + reduced)/100 Chl (mol/mol)	6.0 ± 0.5	8.9 ± 0.4

Comparison of the redox state of the PQ pool, its size and the redox state of the photochemically non-active PQ between wild-type ± and Cr-PTOX1 plants. The data represent the mean ± standard error (SE) of six independent measurements.

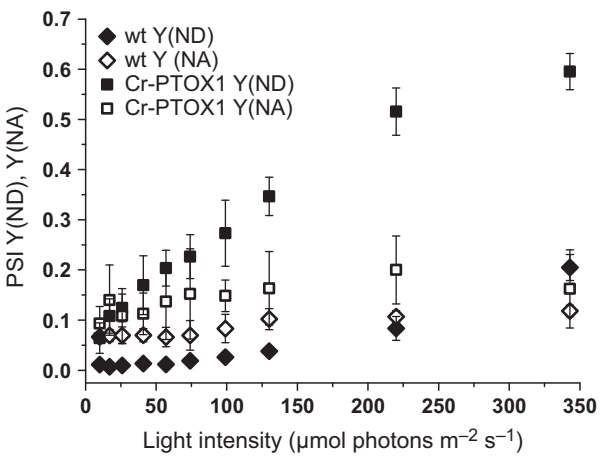

Figure 3. Photosystem I of Cr-PTOX1 plants shows higher donor-side limitation Y(ND).
Light dependency of acceptor [Y(NA)]- and donor side [Y(ND)] limitation of PSI quantum yield. Saturating pulse analysis was used to compare wild-type and Cr-PTOX1 plants using the DUAL-PAM. Filled diamonds: wild-type Y(ND); open diamonds: wild-type Y(NA); filled squares: Cr-PTOX1 Y(ND); open squares: Cr-PTOX1 Y(NA). The data represent the mean ± standard error (SE) of five independent measurements.

CO_2 fixation in Cr-PTOX1 plants and regulation of PTOX activity

The obtained data indicate that linear electron flow is reduced in Cr-PTOX1 plants compared with wild-type, and it was questioned whether these plants produce enough NADPH and ATP for the reduction of CO_2 in the Calvin-Benson-Bassham cycle. When CO_2 assimilation of wild-type and Cr-PTOX1 leaves was measured (Figure 4), Cr-PTOX1 plants fixed about three times less CO_2 compared with wild-type on a leaf area basis under normal CO_2 conditions (400 ppm CO_2). When assimilation rate was expressed not on leaf area but on chlorophyll content, CO_2 fixation rate in Cr-PTOX1 plants was still two times lower compared to wild-type. Low carbohydrate production is in agreement with the retarded growth of Cr-PTOX1 plants and the observation that these plants grew better in continuous light (Figure S1). The shoot and root dry weight of wild-type and Cr-PTOX1 plants were measured and the shoot/root ratio determined (Figure S6). This showed that the shoot/root ratio was higher in Cr-PTOX1 plants than in the wild-type indicating carbohydrate limitation (Ericsson, 1994) and that the sink-source equilibrium was perturbed.

However, increasing the ambient CO_2 level to 2000 ppm abolished the difference between wild-type and Cr-PTOX1 plants when CO_2 assimilation was normalized to chlorophyll (Figure 4b). As elevation of CO_2 is unlikely to affect directly the partition of PQH_2 oxidation between PTOX and cytochrome *b6f* complex, an indirect effect is expected to take place. It is known that elevation of CO_2, besides the repression of photorespiration, leads to a slight acidification of the stroma (Hauser *et al.*, 1995). Since PTOX activity itself is pH-independent in the physiologically relevant pH range (Yu *et al.*, 2014), a change in the pH of the stroma may change the accessibility of PTOX to its substrate PQH_2. If this was the case, PTOX activity would be regulated by its membrane association. To test this hypothesis, the attachment of PTOX to the thylakoid membrane in the wild-type was studied as a function of light-dependent alkalization of the stroma. Leaves of wild-type were incubated in dark and high light, quickly homogenized and separated by centrifugation in a supernatant and a membrane fraction. These fractions were analyzed by SDS-PAGE and immunoblotting. As shown in Figure 5, PTOX was associated to the thylakoid membrane isolated from leaves exposed to high light, but not in those isolated from dark-adapted leaves, where it was found in the supernatant.

DISCUSSION

Using a combined biochemical and biophysical approach, we demonstrated that the additional expression of Cr-PTOX1 increased PTOX activity strongly (Figures 1 and 2) resulting in a more oxidized redox state of the PQ pool (Figure 2 and Table 2). Electron donation to PSI was affected (Figure 3), and the plants suffered from a lack of electron supply for assimilation (Figures 4a and S6). At higher light intensities, plants expressing Cr-PTOX1 suffered from photoinhibition as has been reported earlier for this transformant (Ahmad *et al.*, 2012). Cr-PTOX1 plants produced more $O_2^{\bullet-}/H_2O_2$ (Figure S3, Heyno *et al.*, 2009) indicating that PTOX acts in a pro-oxidant manner. Depending on the plastoquinol concentration, PTOX, besides catalyzing the complete reduction of O_2 to H_2O, generates partially ROS as has been demonstrated *in vitro* using recombinant PTOX from rice (Feilke *et al.*, 2014; Yu *et al.*, 2014). Transformants with increased PTOX levels have been shown to exhibit either no phenotype under photoinhibitory conditions (Rosso *et al.*, 2006) or to exhibit signs of photoinhibition (Heyno *et al.*, 2009; Ahmad *et al.*, 2012). These differences between the available

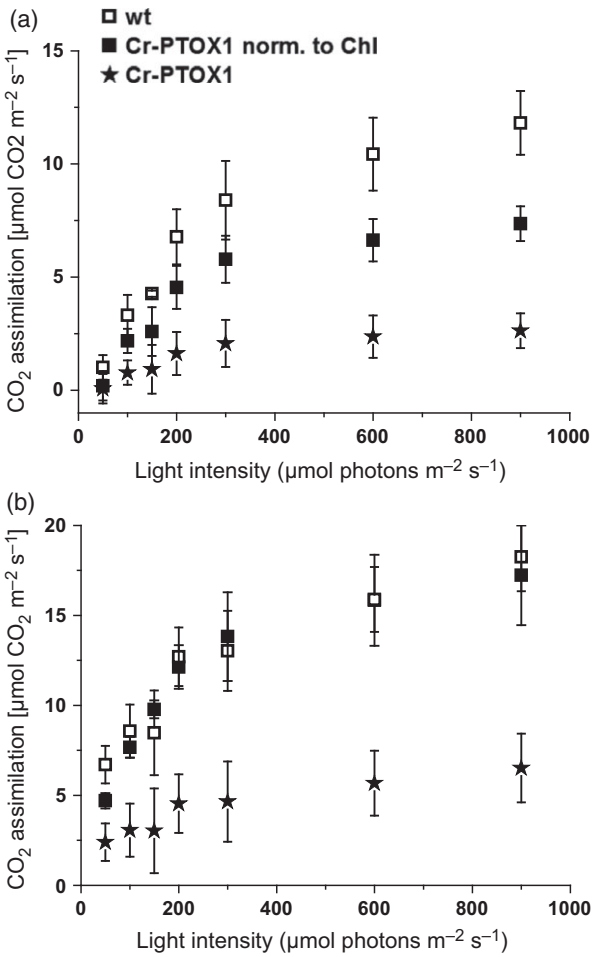

Figure 4. CO_2 assimilation in wild-type and Cr-PTOX1 plants.
The photosynthetic rate of wild-type (open squares) and Cr-PTOX1 plants (filled squares) per leaf area was measured in response to different light intensities. Results obtained with Cr-PTOX1 plants were also normalized to chlorophyll content (asterisks). The data represent the mean ± standard error (SE) of four independent measurements.
(a) CO_2 partial pressure at 400 ppm.
(b) CO_2 partial pressure at 2000 ppm.

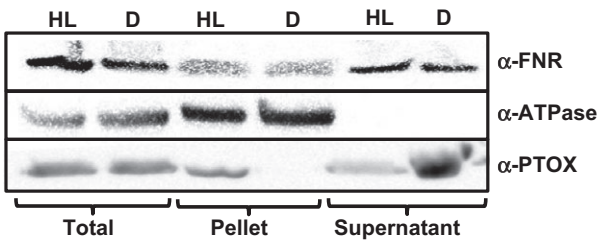

Figure 5. PTOX attachment to the membrane depends on light and pH value.
Leaves of wild-type plants were incubated for 1 h in dark (D) and high light (HL; 500 µmol photons m^{-2} sec^{-1}). PTOX content of total leaf extract (Total), thylakoid membranes (Pellet) and supernatants was analyzed by SDS-PAGE and immunoblotting. As loading control antibodies against the β-subunit of ATP synthase (ATPase) and ferredoxin-NADP reductase (FNR) were used. The density of the PTOX band in the pellet was 60 ± 20% in HL and 7 ± 7% in D when normalized to the density of the band of the β-subunit of ATP synthase [mean ± standard error (SE), three blots, each with proteins from different preparations, were used for the statistical analysis]. Gels were loaded based on protein content.

transformants may simply be due to the expression level of PTOX. PTOX levels are kept rather low in plants grown under normal conditions (1% of PSII level in *A. thaliana,* Lennon *et al.*, 2003), and only plants exposed to abiotic stress show elevated PTOX level (Streb *et al.*, 2005; Quiles, 2006; Díaz *et al.*, 2007; Stepien and Johnson, 2009; Ibáñez *et al.*, 2010; Ivanov *et al.*, 2012; Laureau *et al.*, 2013). Keeping the amount of PTOX low avoids its competition with linear and cyclic electron flow and diminishes unnecessary ROS formation via PTOX. However abiotic stress leads to the downregulation of forward electron transport, and under these conditions active PTOX serves as an alternative electron sink and safety valve.

It is generally accepted that PTOX has a low activity compared with photosynthetic electron flow. The maximum rate of PTOX was reported to be 5 e^- sec^{-1} $PSII^{-1}$ for PTOX2 in *C. reinhardtii* (Houille-Vernes *et al.*, 2011) and 0.3 e^- sec^{-1} $PSII^{-1}$ in tomato (Trouillard *et al.*, 2012) while the maximal rate of photosynthesis is approximately 150 e^- sec^{-1} $PSII^{-1}$ (Nawrocki *et al.*, 2015). These activities are most likely underestimated since PTOX activity was measured by chlorophyll fluorescence using dark-adapted leaves or cells. *In vitro* study of the enzyme activity using recombinant PTOX showed a high activity of the enzyme (up to 19.1 ± 1.1 µmol O_2 mg $protein^{-1}$ min^{-1}; Yu *et al.*, 2014). In addition, the data presented here show that PTOX competes efficiently with photosynthetic electron flow under steady-state conditions (Figures 3 and 4a). The high PTOX protein level (Ahmad *et al.*, 2012) is most likely responsible for the strong competition of Cr-PTOX1 with the photosynthetic electron flow in the transformant rather than special characteristics of PTOX1 from *C. reinhardtii.* In addition, the recovery of NPQ in Cr-PTOX1 plants was slower than in the wild-type (Table 1 and Figure S2). This may be caused by quenching due to photoinhibition, to a slower relaxation of the proton gradient, to differences in state transition or in chloroplast movements in these plants. This observation is in contrast to previous work on cyanobacteria. It has been reported for marine *Synechococcus* that PTOX competes with P700 for electrons while the photochemical efficiency [Φ(II)] remains high when PTOX is active (Bailey *et al.*, 2008). In the case of Cr-PTOX1 expressing plants, it is most likely the unnaturally high Cr-PTOX1 level that leads to a reduced Φ(II) and enhanced photoinhibition.

Acidification of the lumen serves as a key element to down-regulate photosynthetic electron transport. Known mechanisms include NPQ and the photosynthetic control, i.e. the slowing down of PQH_2 by the cytochrome b_6f

complex (Kramer *et al.*, 2004; Foyer *et al.*, 2012). According to the data presented in Figure 5, changes in PTOX activity can be added as a new player to the consortium of pH-dependent regulation mechanisms. In wild-type tobacco PTOX was associated with the membrane only in light-adapted leaves at pH 8.0 while it was found in a soluble form in the supernatant in dark-adapted leaves at pH 6.7. In the dark in the absence of a ΔpH the difference in the intensity of the AG-band (Figure 2c) between wild-type and Cr-PTOX1 plants disappeared. Moreover, high CO_2 leading to an acidification of the stroma abolished the difference in CO_2 assimilation between Cr-PTOX1 plants and the wild-type (Figure 4b). Furthermore, the growth differences between wild-type and Cr-PTOX1 plants became very small when plants were grown under low light conditions (Ahmad *et al.*, 2012). The pH value of the stroma is known to increase upon illumination (Heldt *et al.*, 1973), and the light-induced proton influx is electrically counterbalanced by ion fluxes through Cl^--channels (Schönknecht *et al.*, 1988) and K^+-channels (Tester and Blatt, 1989; Carraretto *et al.*, 2013). We suppose that both, the pH value and the ion concentration, are crucial for the attachment of PTOX to the membrane. According to reconstitution experiments using recombinant Os-PTOX fused with the maltose binding protein, a more alkaline pH and the presence of sodium in comparison to calcium increased the attachment of PTOX to the membrane (Feilke *et al.*, 2014). In the present state, we do not know if the association of PTOX with the membrane changes depending on the pH value or ion concentrations, if the interaction of PTOX with a putative partner protein is interrupted or if alterations of the pH induce a conformational shift in the PTOX protein structure that leads to a dissociation of the protein from the membrane. Another example of an enzyme involved in pH-dependent regulation of photosynthetic electron flow known to associate with the membrane in a pH-dependent manner is the violaxanthin de-epoxidase (Hager and Holocher, 1994; Hieber *et al.*, 2002), and it seems likely that other soluble enzymes of the carotenoid biosynthesis pathway do also associate to the membrane in a ΔpH- or Δψ-dependent manner (Peter Beyer, personal communication).

According to our hypothesis, the pH-dependent localization of PTOX (Figure 5) explains why this enzyme may act as a safety valve protecting against high light or other abiotic stresses. At non-saturating light conditions, the proton gradient across the membrane does not exceed a certain threshold value, and PTOX does not interfere with photosynthetic electron transport. Above this threshold, increase in pH value and ion concentration in the stroma allow the membrane attachment of PTOX and thereby its accessibility to its lipophilic substrate PQH_2. PTOX attaches tightly and oxidizes PQH_2. A highly reduced PQ pool triggers photoinhibition as it increases the probability of charge recombination reactions in PSII leading to triplet chlorophyll formation and to the generation of toxic singlet oxygen. The critical stromal pH value is reached when light intensities exceed CO_2 assimilation, and photosynthetic electron transport and reoxidation of PQH_2 are slowed down at the cytochrome b_6f complex (Kramer *et al.*, 2004; Foyer *et al.*, 2012). This decrease in luminal pH value triggers NPQ which dissipates excess energy and thereby protects the photosynthetic apparatus against light-induced damage. At the same time, PTOX attaches to the membrane and avoids over-reduction of the PQ pool.

EXPERIMENTAL PROCEDURES

Materials

Nicotiana tabacum (var. *Petit havana*) wild-type and the plastid transformant expressing plastid terminal oxidase 1 from the green alga *C. reinhardtii* (Cr-PTOX1; Ahmad *et al.*, 2012) were grown for 4–6 weeks in soil under continuous light (80 μmol photons m^{-2} sec^{-1}, 21°C). Alternatively, plants were grown in a 12 h light/12 h dark period at the same light intensity. For measurements on single leaves, leaves of the same age were used.

Thylakoid membrane preparation from *N. tabacum*

For activity assays leaves were homogenized with a Warring blender for 10 sec in 0.33 M sorbitol, 60 mM KCl, 10 mM EDTA, 1 mM $MgCl_2$, 25 mM MES pH 6.1, and filtrated through four layers of mull. After centrifugation the pellet was first washed with 0.33 M sorbitol, 60 mM KCl, 10 mM EDTA, 1 mM $MgCl_2$, 25 mM HEPES pH 6.7, then resuspended in 5 mM $MgCl_2$, 20 mM HEPES pH 7.6 to break intact chloroplasts. After centrifugation, the pellet was resuspended in 0.3 M sucrose, 5 mM $MgCl_2$, 20 mM HEPES pH 7.6 (measurement buffer) to a final concentration of 1 mg Chl mL^{-1}. All centrifugations were performed at 3000 ***g*** for 3 min at 4°C.

Protein extraction from *N. tabacum*

For immunoblots, leaves were incubated for 1 h in dark or high light (500 μmol photons m^{-2} sec^{-1}). After short homogenization (10 sec) in buffer [0.33 M sorbitol, 60 mM KCl, 10 mM EDTA, 1 mM $MgCl_2$, 25 mM HEPES and protease inhibitor cocktail (Sigma-Aldrich, St Louis, Missouri, USA)] and filtration through four layers of mull, a part was removed for the total extract and the rest was separated by centrifugation (5 min, 3000 ***g*** at 4°C) in a supernatant and a membrane fraction. For dark-incubated sample, the pH value of the buffer was set to 6.7, while for high light-incubated leaves, the pH value was set to 8.0. Proteins in the supernatant were precipitated with 10% trichloroacetic acid; the pellet was washed twice with ice-cold acetone and desiccated.

Pigment analysis

Leaves were ground in liquid nitrogen and subsequently extracted by acetone containing 0.01% ammoniac, the extracts were pooled and evaporated to dryness, then resuspended in 200 μL acetone. Analysis was conducted using a Shimadzu UFLC HPLC chain (Shimadzu, Marne-la-Vallée, France), including LC-20AD pumps, a SIL-20AC HT sample manager, a CTO-20A column oven, a UVSPD-M20A DAD-UV detector. Carotenoids and chlorophylls were separated on a 150 × 4.6 mm i.d., 5 μm, reverse-phase VisionHT C18 HL C18 column (Grace, Epernon, France) using solvent A, ethyl acetate 100% (0.5% acetic acid), and solvent B, water/acetonitrile (10:90, v/v, 0.5% acetic acid), with a gradient profile (from 10% to

95% A) and 0.5 mL min^{-1} flow rate. Detection was set to 450 nm. Carotenoids were identified on the basis of their absorption spectra and quantified with external standard calibration.

Photosystem I and II activity assays

Measurements of O_2 evolution and consumption in thylakoids were performed in a Liquid-Phase Oxygen Electrode Chamber (Hansatech Instruments, Norfolk, UK). PSII activity was measured as O_2 evolution in the presence of 1 mM 2,6-dichloro-1,4-benzoquinone. PSI activity was measured as O_2 consumption in the presence of 10 μM 3-(3,4-dichlorophenyl)-1,1-dimethylurea (DCMU), 5 mM ascorbate, 30 μM 2,6-dichlorophenol-indophenol and 500 μM methylviologen. All measurements were performed in the presence of 10 mM NH_4Cl as uncoupler.

Room temperature chlorophyll *a* fluorescence

Room temperature chlorophyll fluorescence was measured using a pulse-amplitude modulation fluorometer (DUAL or IMAGING-PAM, Walz, Effeltrich, Germany). As actinic light, red light at 635 nm was used. The intensity of the measuring light was sufficiently low so that no increase in the fluorescence (F_0) was observed upon set-on of the measuring light. Thylakoids (20 μg Chl ml^{-1}) were dark-adapted for 3 min. When indicated, DCMU was added (10 μM final concentration) to block the electron transfer from Q_A to Q_B.

Plants were taken from the growth chamber during the light period and dark-adapted for 10 min prior to the measurement to allow most of the reversible quenching to relax. The maximum fluorescence level, F_m, was obtained using a saturating flash (600 msec, 10 000 μmol photons m^{-2} sec^{-1}). The maximum quantum yield of PSII, F_v/F_m, was assayed by calculating the ratio of the variable fluorescence, F_v, to the maximal fluorescence, Fm, in the dark-adapted state. PS II quantum yield (Φ_{PSII}), photochemical (qP) and NPQ were assayed during 10 min of actinic light (95 or 340 μmol photons m^{-2} sec^{-1}). Φ_{PSII} was defined as $(F_m' - F)/F_m'$, qP as $(F_m' - F)/(F_m - F_0')$ and NPQ as $F_m - F_m'/F_m'$ with F_m' being the maximal fluorescence in the actinic light.

77K fluorescence emission

Leaves were taken from growth light (I = 80 μmol photons m^{-2} sec^{-1}) or illuminated with far-red light (I = 480 μmol photons m^{-2} sec^{-1}) for 10 min and then frozen in liquid nitrogen. A leaf powder was prepared and resuspended in 0.3 M sucrose, 5 mM $MgCl_2$, 20 mM HEPES pH 7.6. Fluorescence emission spectra at 77K were monitored in a CARY Eclipse spectrophotometer (Varian, Agilent, Santa Clara, CA, USA) equipped with a Dewar. Samples were excited at 435 nm, and the emission was recorded between 650 and 800 nm. For analysis the ratio of PSI/PSII was determined by integrating the peaks at 685 nm and 730 nm.

Spin-trapping electron paramagnetic resonance (EPR) spectroscopy

Spin-trapping assays with 4-pyridyl-1-oxide-*N*-*tert*-butylnitrone (4-POBN) (Sigma-Aldrich, MO, USA) to detect the formation of hydroxyl radicals were carried out using leaf discs. Samples were illuminated for 1 h with white growth or high light (80 or 500 μmol photons m^{-2} sec^{-1}) in the presence of 50 mM 4-POBN, 4% ethanol, 50 μM Fe-EDTA, and buffer (20 mM phosphate buffer, pH 7.5, 5 mM $MgCl_2$ and 0.3 M sorbitol). EPR spectra were recorded at room temperature in a standard quartz flat cell using an EPR e-scan spectrometer (Bruker, Rheinstetten, Germany). The following parameters were used: microwave frequency 9.74 GHz, modulation frequency 86 kHz, modulation amplitude 1 G, microwave power 4.45 mW, receiver gain 5×10^2, time constant 40.96 msec; number of scans 4.

P_{700} measurements

The redox state of P_{700} was monitored by following differences of the 875 nm and 830 nm transmittance signals using a DUAL-PAM (Walz, Effeltrich, Germany) and leaves of intact plants. The plants were kept in the light in the growth chamber so that the Calvin–Benson cycle enzymes were active. Kinetics of P_{700} oxidation were probed by far-red illumination according to Joliot and Johnson (2011). For this assay, plants were dark-adapted for 10 min, then preilluminated for 5 min with far-red light. After this pre-illumination the P_{700} measurement was started using the following illumination protocol: 5 sec actinic red light (600 μmol photons m^{-2} sec^{-1}), 2 sec dark, 17 sec far-red light (480 μmol photons m^{-2} sec^{-1}, highest intensity of the DUAL-PAM). Only the first seconds after onset of far-red light are shown in Figure 1(b). The amplitudes of the signals were normalized to 1.

To measure the P_{700} light curve and determine quantum yields of PSI donor (Y(ND)) and acceptor side-limitations (Y(NA), saturating pulse analysis was used. After the determination of maximal P_{700} oxidation the leaf was illuminated stepwise 5 min at increasing light intensities from 10 to 343 μmol photons m^{-2} sec^{-1}. A saturating pulse was applied at the end of each light step for determination of P700 Y(NA) and Y(ND).

Measurements of the size of the PQ pool and its redox state

The size and the redox state of the PQ pool were estimated using HPLC as described by Kruk and Karpinski (2006). In short, the leaf disks of saturating light-treated, DCMU-treated and from growth light conditions were homogenized quickly in ethyl acetate and after evaporation, the extracts were analyzed by HPLC where the level of both oxidized and reduced forms of PQ was determined. From these data, the size and the redox state of the PQ pool, as well as the size and the redox state of photochemically non-active PQ was calculated as described in Kruk and Karpinski (2006).

Thermoluminescence

Thermoluminescence was measured with a home-built apparatus on leaf segments taken from plants dark-adapted for 2 min with a home-built apparatus (Krieger *et al.*, 1998). Thermoluminescence was excited at 1°C with a single-turnover flash (Xenon flash lamp, Walz, Effeltrich), three single-turnover flashes spaced with 1 sec dark interval or for 30 sec with saturating far-red light. Samples were heated at a rate of 0.4° sec^{-1} to 70°C and the light emission was recorded.

Gas exchange and chlorophyll *a* fluorescence measurements

Net CO_2 uptake by leaves in combination with chlorophyll fluorescence emission was measured using a LI-6400 (Li-Cor Inc., Lincoln, NE, USA) equipped with a leaf chamber fluorometer 6400–40 essentially as described by Priault (Priault *et al.*, 2006). Oxygen evolution was determined with a Hansatech oxygen electrode and a LD2 chamber (Hansatech Instruments Ltd, Kings Lynn, UK) as described by Streb, Feierabend and Bligny (Streb *et al.*, 1997). Intact plants in pots were transferred in the morning to the laboratory. After insertion of attached leaves into the leaf chamber

(2 cm^2), leaves were dark adapted for at least 30 min to measure dark respiration, minimum fluorescence yield (F_o) and maximum fluorescence yield (F_m). Afterwards, leaves were acclimated to 300 μmol photons m^{-2} sec^{-1}. The whole Li-Cor leaf chamber was maintained in a second closed-thermostated chamber to avoid any external gas exchange. Measurements were done at leaf temperatures between 22 and 23°C and at a leaf water pressure deficit of approximately 1 kPa in an atmosphere of 21% oxygen and 400 or 2000 ppm carbon dioxygen.

Immunoblots

Total leaf extract, supernatant and pellet were prepared as described above and used for analysis by SDS-PAGE (10% acrylamide) and immunoblotting. Proteins were blotted onto a nitrocellulose membrane. Labelling of the membranes with anti-PTOX antibody, anti-ATPase antibody (β-subunit of ATP synthase; Agrisera, Vännäs, Sweden) or anti-FNR antibody (ferredoxin–NADP reductase) was carried out at room temperature in 50 mM Tris–HCl pH 7.6, 150 mM NaCl, 0.1% Tween-20 and 5% non-fat milk powder. After washing, bound antibodies were revealed with a peroxidase-linked secondary anti-rabbit antibody (Agrisera, Vännäs, Sweden) and visualized by enhanced chemiluminescence.

ACKNOWLEDGEMENTS

We thank P. Nixon (Imperial College London) for providing us with Cr-PTOX1 seeds, M. Kuntz (University Grenoble) and W. Oettmeier (University Bochum) for the generous gift of anti-PTOX antibody and anti-FNR-antibody, respectively. This work was supported by the CNRS, the CEA and the Université Paris-Sud.

SUPPORTING INFORMATION

Additional Supporting Information may be found in the online version of this article.

Figure S1. Tolerance of wild-type and Cr-PTOX1 plants to different light periods.

Figure S2. Chlorophyll fluorescence quenching analysis of wild-type and Cr-PTOX1 leaves.

Figure S3. Light induced hydroxyl radical formation in wild-type and Cr-PTOX1 leaf discs.

Figure S4. 77K fluorescence emission spectra from wild-type and Cr-PTOX1 leaves.

Figure S5. Immunoblot of leaf extracts from wt and Cr-PTOX1 plants.

Figure S6. Cr-PTOX1 plants show a higher shoot/root ratio.

REFERENCES

Ahmad, N., Michoux, F. and Nixon, P.J. (2012) Investigating the production of foreign membrane proteins in tobacco chloroplasts: expression of an algal plastid terminal oxidase. *PLoS ONE*, **7**, e41722.

Aluru, M.R. and Rodermel, S.R. (2004) Control of chloroplast redox by the IMMUTANS terminal oxidase. *Physiol. Plant.* **120**, 4–11.

Bailey, S., Melis, A., Mackey, K.R.M., Cardol, P., Finazzi, G., van Dijken, G., Berg, G.M., Arrigo, K., Shrager, J. and Grossman, A. (2008) Alternative photosynthetic electron flow to oxygen in marine Synechococcus. *Biochim. Biophys. Acta*, **1777**, 269–276.

Berthold, D.A., Andersson, M.E. and Nordlund, P. (2000) New insight into the structure and function of the alternative oxidase. *Biochim. Biophys. Acta*, **1460**, 241–254.

Carol, P., Stevenson, D., Bisanz, C., Breitenbach, J., Sandmann, G., Mache, R., Coupland, G. and Kuntz, M. (1999) Mutations in the Arabidopsis gene IMMUTANS cause a variegated phenotype by inactivating a chloroplast terminal oxidase associated with phytoene desaturation. *Plant Cell*, **11**, 57–68.

Carraretto, L., Formentin, E., Teardo, E., Checchetto, V., Tomizioli, M., Morosinotto, T., Giacometti, G.M., Finazzi, G. and Szabó, I. (2013) A thylakoid-located two-pore K^+ channel controls photosynthetic light utilization in plants. *Science*, **342**, 114–118.

Díaz, M., de Haro, V., Muñoz, R. and Quiles, M.J. (2007) Chlororespiration is involved in the adaptation of *Brassica* plants to heat and high light intensity. *Plant, Cell Environ.* **30**, 1578–1585.

Ericsson, T. (1994) Growth and shoot: root ratio of seedlings in relation to nutrient availability. *Plant Soil*, **168–169**, 205–214.

Feilke, K., Yu, Q., Beyer, P., Sétif, P. and Krieger-Liszkay, A. (2014) *In vitro* analysis of the plastid terminal oxidase in photosynthetic electron transport. *Biochim. Biophys. Acta*, **1837**, 1684–1690.

Foyer, C.H., Neukermans, J., Queval, G., Noctor, G. and Harbinson, J. (2012) Photosynthetic control of electron transport and the regulation of gene expression. *J. Exp. Bot.* **63**, 1637–1661.

Fu, A., Park, S. and Rodermel, S. (2005) Sequences required for the activity of PTOX (IMMUTANS), a plastid terminal oxidase *in vitro* and *in planta* mutagenesis of iron-binding sites and a conserved sequence that corresponds to exon 8. *J. Biol. Chem.* **280**, 42489–42496.

Hager, A. and Holocher, K. (1994) Localization of the xanthophyll-cycle enzyme violaxanthin de-epoxidase within the thylakoid lumen and abolition of its mobility by a (light-dependent) pH decrease. *Planta*, **192**, 581–589.

Hauser, M., Eichelmann, H., Oja, V., Heber, U. and Laisk, A. (1995) Stimulation by light of rapid pH Regulation in the chloroplast stroma *in vivo* as Indicated by CO_2 solubilization in leaves. *Plant Physiol.* **108**, 1059–1066.

Heldt, H.W., Werdan, K., Milovancev, M. and Geller, G. (1973) Alkalization of the chloroplast stroma caused by light-dependent proton flux into the thylakoid space. *Biochim. Biophys. Acta*, **314**, 224–241.

Hernández, J.A., Corpas, F.J., Gómez, M., del Río, L.A. and Sevilla, F. (1993) Salt-induced oxidative stress mediated by activated oxygen species in pea leaf mitochondria. *Physiol. Plant.* **89**, 103–110.

Heyno, E., Gross, C.M., Laureau, C., Culcasi, M., Pietri, S. and Krieger-Liszkay, A. (2009) Plastid alternative oxidase (PTOX) promotes oxidative stress when overexpressed in tobacco. *J. Biol. Chem.* **284**, 31174–31180.

Hieber, A.D., Bugos, R.C., Verhoeven, A.S. and Yamamoto, H.Y. (2002) Overexpression of violaxanthin de-epoxidase: properties of C-terminal deletions on activity and pH-dependent lipid binding. *Planta*, **214**, 476–483.

Houille-Vernes, L., Rappaport, F., Wollman, F.A., Alric, J. and Johnson, X. (2011) Plastid Terminal Oxidase 2 (PTOX2) is the major oxidase involved in chlororespiration in *Chlamydomonas*. *Proc. Natl Acad. Sci. USA*, **108**, 20820–20825.

Ibáñez, H., Ballester, A., Muñoz, R. and José Quiles, M. (2010) Chlororespiration and tolerance to drought, heat and high illumination. *J. Plant Physiol.* **167**, 732–738.

Ivanov, A.G., Rosso, D., Savitch, L.V., Stachula, P., Rosembert, M., Oquist, G., Hurry, V. and Hüner, N.P.A. (2012) Implications of alternative electron sinks in increased resistance of PSII and PSI photochemistry to high light stress in cold-acclimated *Arabidopsis thaliana*. *Photosynth. Res.* **113**, 191–206.

Joët, T., Genty, B., Josse, E.M., Kuntz, M., Cournac, L. and Peltier, G. (2002) Involvement of a plastid terminal oxidase in plastoquinone oxidation as evidenced by expression of the *Arabidopsis thaliana* enzyme in tobacco. *J. Biol. Chem.* **277**, 31623–31630.

Joliot, P. and Johnson, G.N. (2011) Regulation of cyclic and linear electron flow in higher plants. *Proc. Natl Acad. Sci. USA*, **108**, 13317–13322.

Josse, E.-M., Alcaraz, J.-P., Labouré, A.-M. and Kuntz, M. (2003) *In vitro* characterization of a plastid terminal oxidase (PTOX). *Eur. J. Biochem.* **270**, 3787–3794.

Kramer, D.M., Avenson, T.J. and Edwards, G.E. (2004) Dynamic flexibility in the light reactions of photosynthesis governed by both electron and proton transfer reactions. *Trends Plant Sci.* **9**, 349–357.

Krieger, A., Bolte, S., Dietz, K.-J. and Ducruet, J.-M. (1998) Thermoluminescence studies on the facultative crassulacean-acid- metabolism plant *Mesembryanthemum crystallinum* L. *Planta*, **205**, 587–594.

Krieger-Liszkay, A. (2005) Singlet oxygen production in photosynthesis. *J. Exp. Bot.* **56**, 337–346.

Kruk, J. and Karpinski, S. (2006) An HPLC-based method of estimation of the total redox state of plastoquinone in chloroplasts, the size of the photochemically active plastoquinone-pool and its redox state in thylakoids of Arabidopsis. *Biochim. Biophys. Acta*, **1757**, 1669–1675.

Kuntz, M. (2004) Plastid terminal oxidase and its biological significance. *Planta*, **218**, 896–899.

Laureau, C., De Paepe, R., Latouche, G., Moreno-Chacón, M., Finazzi, G., Kuntz, M., Cornic, G. and Streb, P. (2013) Plastid terminal oxidase (PTOX) has the potential to act as a safety valve for excess excitation energy in the alpine plant species *Ranunculus glacialis* L. *Plant, Cell Environ.* **36**, 1296–1310.

Lennon, A.M., Prommeenate, P. and Nixon, P.J. (2003) Location, expression and orientation of the putative chlororespiratory enzymes, ndh and immutans, in higher-plant plastids. *Planta*, **218**, 254–260.

Munné-Bosch, S. and Alegre, L. (2002) The function of tocopherols and tocotrienols in plants. *Crit. Rev. Plant Sci.* **21**, 31–57.

Nambara, E. and Marion-Poll, A. (2005) Abscisic acid biosynthesis and catabolism. *Annu. Rev. Plant Biol.* **56**, 165–185.

Nawrocki, W.J., Tourasse, N.J., Taly, A., Rappaport, F. and Wollman, F.-A. (2015) The plastid terminal oxidase: its elusive function points to multiple contributions to plastid physiology. *Annu. Rev. Plant Biol.* **66**, 49–74.

Nordby, H.E. and Yelenosky, G. (1985) Change in citrus leaf lipids during freeze-thaw stress. *Phytochemistry*, **24**, 1675–1679.

Priault, P., Tcherkez, G., Cornic, G., Paepe, R.D., Naik, R., Ghashghaie, J. and Streb, P. (2006) The lack of mitochondrial complex I in a CMSII mutant of *Nicotiana sylvestris* increases photorespiration through an increased internal resistance to CO_2 diffusion. *J. Exp. Bot.* **57**, 3195–3207.

Quiles, M.J. (2006) Stimulation of chlororespiration by heat and high light intensity in oat plants. *Plant, Cell Environ.* **29**, 1463–1470.

Roncel, M. and Ortega, J.M. (2005) Afterglow thermoluminescence band as a possible early indicator of changes in the photosynthetic electron transport in leaves. *Photosynth. Res.* **84**, 167–172.

Rosso, D., Ivanov, A.G., Fu, A. *et al.* (2006) IMMUTANS does not act as a stress-induced safety valve in the protection of the photosynthetic apparatus of Arabidopsis during steady-state photosynthesis. *Plant Physiol.* **142**, 574–585.

Rumeau, D., Peltier, G. and Cournac, L. (2007) Chlororespiration and cyclic electron flow around PSI during photosynthesis and plant stress response. *Plant, Cell Environ.* **30**, 1041–1051.

Schönknecht, G., Hedrich, R., Junge, W. and Raschke, K. (1988) A voltage-dependent chloride channel in the photosynthetic membrane of a higher plant. *Nature*, **336**, 589–592.

Shahbazi, M., Gilbert, M., Labouré, A.-M. and Kuntz, M. (2007) Dual role of the plastid terminal oxidase in tomato. *Plant Physiol.* **145**, 691–702.

Stepien, P. and Johnson, G.N. (2009) Contrasting responses of photosynthesis to salt stress in the glycophyte Arabidopsis and the halophyte *Thellungiella*: role of the plastid terminal oxidase as an alternative electron sink. *Plant Physiol.* **149**, 1154–1165.

Streb, P., Feierabend, J. and Bligny, R. (1997) Resistance to photoinhibition of photosystem II and catalase and antioxidative protection in high mountain plants. *Plant, Cell Environ.* **20**, 1030–1040.

Streb, P., Josse, E.-M., Gallouët, E., Baptist, F., Kuntz, M. and Cornic, G. (2005) Evidence for alternative electron sinks to photosynthetic carbon assimilation in the high mountain plant species *Ranunculus glacialis*. *Plant, Cell Environ.* **28**, 1123–1135.

Szymańska, R. and Kruk, J. (2010) Plastoquinol is the main prenyllipid synthesized during acclimation to high light conditions in Arabidopsis and is converted to plastochromanol by tocopherol cyclase. *Plant Cell Physiol.* **51**, 537–545.

Tester, M. and Blatt, M.R. (1989) Direct measurement of k channels in thylakoid membranes by incorporation of vesicles into planar lipid bilayers. *Plant Physiol.* **91**, 249–252.

Trouillard, M., Shahbazi, M., Moyet, L., Rappaport, F. and Joliot, P.A. (2012) Kinetic properties and physiological role of the plastoquinone terminal oxidase (PTOX) in a vascular plant. *Biochim. Biophys. Acta*, **1817**, 2140–2148.

Wetzel, C.M., Jiang, C.-Z., Meehan, L.J., Voytas, D.F. and Rodermel, S.R. (1994) Nuclear—organelle interactions: the immutans variegation mutant of Arabidopsis is plastid autonomous and impaired in carotenoid biosynthesis. *Plant J.* **6**, 161–175.

Wu, D., Wright, D.A., Wetzel, C., Voytas, D.F. and Rodermel, S. (1999) The IMMUTANS variegation locus of Arabidopsis defines a mitochondrial alternative oxidase homolog that functions during early chloroplast biogenesis. *Plant Cell*, **11**, 43–55.

Yu, Q., Feilke, K., Krieger-Liszkay, A. and Beyer, P. (2014) Functional and molecular characterization of plastid terminal oxidase from rice (*Oryza sativa*). *Biochim. Biophys. Acta*, **1837**, 1284–1292.